PAPER

Direct spectroscopic evidence for the high-spin state of dioxidomanganese(v)†

Olesya S. Ablyasova, [ID] [ab] Vicente Zamudio-Bayer, [ID] [a] Max Flach, [ID] [ab] Mayara da Silva Santos, [ID] [ab] J. Tobias Lau [ID] [ab] and Konstantin Hirsch [ID] *[a]

The spin state of metal centers in many catalytic reactions has been demonstrated to be a rate limiting factor when high-valent metal centers such as manganese are involved. Although numerous manganese(v) complexes, including a few manganese(v) oxo complexes, have been identified, thus far only one of these, [Mn^{V}H$_3$ buea(O)], has been directly confirmed to exist in a high spin state. Such a high-spin manganese(v) center may play a crucial role in the dioxygen formation process in the elusive S$_4$ state of the Kok cycle in photosystem II. In this study, we provide direct experimental evidence, using X-ray magnetic circular dichroism (XMCD) and X-ray absorption spectroscopy (XAS), of gas phase [OMnO]$^+$ as the second known high-spin manganese(v) oxo complex. We conclusively assign the ground state as ^{3}B$_1$ (C_{2v}). Additionally, we provide fingerprint spectra not only for [OMn^{V}O]$^+$, but also for the high-spin hydroxidooxidomanganese(iv) ion [OMn^{IV}OH]$^+$ in its ^{4}A″ (C_s) ground state that is expected to exhibit similar XAS and XMCD spectral signatures to neutral dioxidomanganese(iv).

1 Introduction

High valent metal-oxo intermediates are believed to be key in facilitating numerous biological and abiotic catalytic oxidation reactions.[1] There is also evidence that the spin state of these high-valent metal-oxo complexes determines their reactivity.[1–5] For example, a combined theoretical and experimental study suggests that the catalytic hydrocarbon oxidation is only facilitated *via* the triplet state of a manganese(v)-oxo complex while the singlet state of that same species is inactive.[6] Moreover, high-spin manganese(v) was also proposed to play a key role in water splitting as the main active site of the oxygen-evolving complex (OEC) of photosystem II.[7–11] Despite the apparent importance of high-valent–high-spin manganese centers, only very few manganese(v)-oxo complexes are known,[6,12–14] most of which are of tetragonal symmetry resulting in a quenched spin magnetic moment. To the best of our knowledge, only one manganese(v)-oxo complex, [Mn^{V}H$_3$buea(O)], that exists in a high-spin (triplet) state has been reported thus far.[15,16] This triplet state has been achieved by tailoring a trigonal ligand symmetry that results in a finite spin at the manganese site.

Previously, we reported on cationic manganese oxide clusters, including [OMnO]$^+$ for which we experimentally and theoretically determined the +5 oxidation state.[13] The comparison of the spectral shape with the computational X-ray absorption spectroscopy (XAS) signature of [OMn^{V}O]$^+$ hinted at a high-spin ^{3}B$_1$ ground state, in line with a calculated high-spin ground state. Here, we present X-ray magnetic circular dichroism (XMCD) spectroscopy of [OMnO]$^+$ that allows direct probing of the magnetic moments of gas-phase ions.[17] By this, we now show conclusively that [OMnO]$^+$ is indeed the second reported high-spin manganese(v)oxo species. Because manganese in oxidation states +5 and +4 might play a pivotal role in the oxygen evolution reaction mediated by the OEC,[7,8,10,11] we provide fingerprint XAS and XMCD spectra, as well as median excitation energies of [OMn^{V}O]$^+$ and [OMn^{IV}OH]$^+$ whose oxidation states are determined by chemical shifts. Locally at the manganese site, the latter exhibits almost the same symmetry as the neutral OMn^{IV}O complex.

2 Methods

XMCD spectroscopy was carried out at the ion trap end station,[18–21] located at beamline UE52-PGM of the synchrotron facility BESSY II operated by Helmholtz-Zentrum Berlin. Dioxidomanganese and hydroxidooxidomanganese cations are produced by DC-sputtering of a manganese target in a helium and argon atmosphere while simultaneously introducing trace amounts of oxygen to the discharge in presence of residual

[a] Abteilung für Hochempfindliche Röntgenspektroskopie, Helmholtz-Zentrum Berlin für Materialien und Energie, Albert-Einstein-Str. 15, Berlin 12489, Germany. E-mail: Konstantin.Hirsch@helmholtz-berlin.de

[b] Physikalisches Institut, Albert-Ludwigs-Universität Freiburg, Hermann-Herder-Str. 3, Freiburg 79104, Germany

† Electronic supplementary information (ESI) available. See DOI: https://doi.org/10.1039/d3cp05468c

5830 | *Phys. Chem. Chem. Phys.*, 2024, **26**, 5830–5835

This journal is © the Owner Societies 2024

water vapour. The ion beam is then guided *via* a hexapole ion guide and quadrupole mass filter, selecting the species of interest, to a liquid-helium cooled quadrupole ion trap for cooling of the clusters to a typical temperature of approximately 20 K. A superconducting solenoid creates a homogeneous magnetic field of $\mu_B H$ = 4.5 T along the trap axis to magnetize the sample. Ion yield (action) spectroscopy is performed by collecting product ions resulting from X-ray absorption of photons with helicity parallel and antiparallel to the magnetic field axis, respectively.[17] Photon energy calibration was performed using the neon 1s excitation in the beamline ionization cell and checked at the oxygen K-edge, giving a photon energy uncertainty of ±0.1 eV. Crystal field and charge transfer multiplet (CF/CTM) simulations were carried out using the program package CTM4XAS (version 5.5),[22] and multiplet ligand-field theory calculations were performed using the software package Xclaim.[23] Density functional theory (DFT) calculations were carried out using ORCA version 4.2.1[24] and turbomole version 7.6.1 employing the B3LYP functional[25,26] and def2-TZVP basis set.[27] Search for the $[OMn^{IV}OH]^+$ ground state structure was performed starting from the reported $[OMn^VO]^+$ ground state structure[13] adding a hydrogen atom either at the manganese or oxygen site, respectively. See the ESI† for details.

3 Results and discussion

3.1 Spin ground state of dioxidomanganese(v) cation

The experimental X-ray absorption spectrum of the $[OMn^VO]^+$ complex at the manganese $L_{2,3}$ edge is shown in the top panel of Fig. 1(a) reproducing the data presented earlier[13] despite being collected on different ion yield channels, namely O^+ here and

Mn^{2+} in the earlier study.[13] From the median L_3 excitation energy of 642.6 ± 0.2 eV, also shown in Fig. 1(a) as a dashed black line, we can deduce the oxidation state[28] of the manganese center in $[OMnO]^+$ to be +5 in agreement with the earlier report,[13] *cf.* ESI,† Fig. S11. The oxidation state assignment is further substantiated by a DFT Mulliken 3d spin population of 2.2 which is known to correlate with the oxidation state in manganese.[29]

In the lower panel of Fig. 1(a) the XMCD signal is presented, which is the difference in X-ray absorption with helicity of the X-ray beam parallel and antiparallel to the magnetic field axis. Additionally, we present the XMCD integral in the lower panel of Fig. 1(a). The XMCD orbital sum rule[30–32] directly links the XMCD integral over both, L_3 and L_2, edges to the expectation value of the orbital magnetic moment at the manganese center. As can be seen, the integral over both $L_{2,3}$-edges approaches zero, indicating a vanishing orbital magnetic moment. A quantitative analysis using the orbital XMCD sum rule[30] yields an orbital magnetization of μ_L = 0.01 ± $0.05\mu_B$ per electron hole. This agrees with quenching of the orbital magnetic moment as is expected in C_{2v} symmetry.[33] Hence, the dichroic signal observed is of pure spin character. Since the manganese center has been shown to be in oxidation state +5, which is equivalent to a nominal local $3d^2$ electron configuration at the manganese site, the non-vanishing XMCD signal, arising from spin only, is evidence for a triplet state. We have therefore experimentally and unambiguously demonstrated that the ground state of the high-valent $[OMn^VO]^+$ complex is a high spin $^3B_1$ (C_{2v}) state.

3.2 XAS and XMCD spectral fingerprinting of $[OMn^VO]^+$ and $[OMn^{IV}OH]^+$

In our special case of $[OMn^VO]^+$ there is no need to further analyse the spectral shape of the L-edge absorption in order to
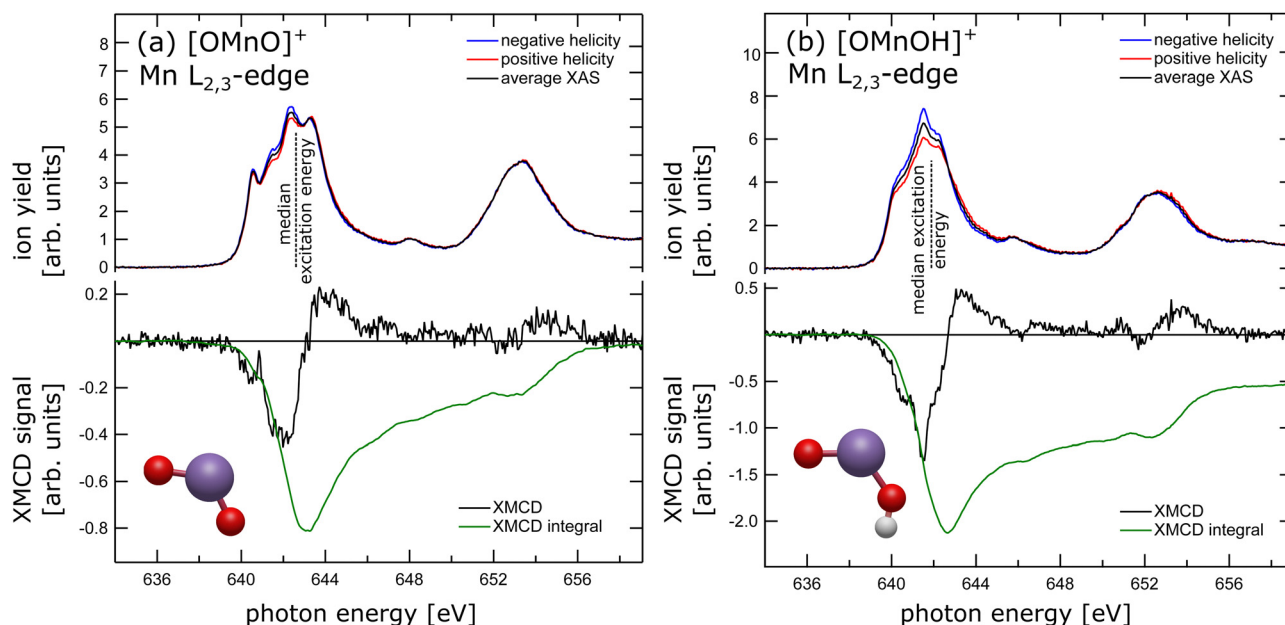
Fig. 1 X-ray absorption spectra (upper panel) recorded with negative (blue trace) and positive (red trace) helicity with respect to the magnetic field axis, and average XAS (black trace) taken at an energy resolution of 170 meV of (a) $[OMn^VO]^+$ and (b) $[OMn^{IV}OH]^+$ complexes. The dashed lines indicate the median L_3 excitation energies of 642.6 ± 0.2 eV and 641.9 ± 0.3 eV, respectively. Lower panel: Experimental XMCD signal (black trace) along with its integral (green trace) of (a) $[OMn^VO]^+$ and (b) $[OMn^{IV}OH]^+$ complexes.

This journal is © the Owner Societies 2024

Phys. Chem. Chem. Phys., 2024, **26**, 5830–5835 | **5831**

extract information on the electronic ground state. However, fingerprinting of the $L_{2,3}$-edge multiplet structure is often successfully employed to determine the electronic configuration of 3d metals and their compounds.[34–38] Additionally, in case of early or high-valent transition metals, the XMCD spin sum rule breaks down[39] and fingerprinting of the XMCD signal is the only fallback option to extract information on the spin state from helicity dependent L-edge absorption. Furthermore, modelling the spectral shape also allows to extract semi-empirical parameters such as the crystal field strength induced by the coordinating ligands.[38]

We therefore employed crystal field and charge transfer multiplet modelling of both XAS and XMCD spectral signatures of the $[OMnO]^+$ complex. However, despite searching a wide parameter space starting from parameters reported for other $3d^2$ systems, namely VI_3[40,41] and FeV_2O_4,[42] the agreement between experiment and simulation is rather poor as can be seen from ESI,† Fig. S1–S6. It is worthwhile mentioning that even wave-function based theoretical models struggle to reproduce all the features of systems exhibiting a $3d^2$ electron configuration.[43] Moreover, the agreement between XAS and XMCD signatures of $[OMn^VO]^+$ with the reported experimental XAS and XMCD signatures of $3d^2$ systems[40–42] is subpar. For a thorough overview of the CF/CTM simulations and a comparison of $[OMn^VO]^+$ XAS and XMCD to reports for VI_3[40,41] or FeV_2O_4[42] see the ESI.† Interestingly, we find a similarly satisfying agreement of the $[OMn^VO]^+$ XMCD signal with that of CrI_3, as can be seen from ESI,† Fig. S8, where the metal center, however, exhibits a $3d^3$ local electronic configuration.[44,45] This seems to indicate that spectral fingerprinting might not be robust for high-valent manganese systems.[46]

In order to test this hypothesis we have prepared manganese in oxidation state +4 in a similar local symmetry by reducing the $[OMn^VO]^+$ complex using residual water and forming the hydroxidooxido manganese(IV) cation, $[OMn^{IV}OH]^+$. Its manganese $L_{2,3}$-edge X-ray absorption spectrum is shown in the upper panel of Fig. 1(b) alongside the median L_3 excitation energy indicated by the dashed line and its ground state geometry as identified by DFT. For related manganese oxide species the shift of the median L_3 excitation energy has been shown to be 0.95 ± 0.02 eV per unit oxidation state.[13] Here, we report the median L_3 excitation energy of $[OMn^{IV}OH]^+$ as 641.9 ± 0.3 eV, *i.e.*, 1.1 eV below and 0.9 eV above the median L_3 excitation energy of Mn^V and Mn^{III} centers, respectively.[13] This reveals an oxidation state of the manganese center in $[OMn^{IV}OH]^+$ of +4 or, put differently, a local $3d^3$ electron configuration. The spins of these three 3d electrons can couple to give either doublet or quartet spin states. Although application of the XMCD spin sum rule in this instance would result in a significant error,[39] comparison of the XMCD intensity of $[OMn^{IV}OH]^+$ as presented in the lower panel of Fig. 1(b) to that of $[OMn^VO]^+$ allows for exclusion of one of the potential spin states of $[OMn^{IV}OH]^+$. Since the XMCD signal of $[OMn^{IV}OH]^+$ is larger by a factor of 3 compared to that of $^3B_1$ (C_{2v}) $[OMn^VO]^+$ this is evidence for $[OMn^{IV}OH]^+$ to be in a quartet spin state. Furthermore, the XMCD integral over both $L_{2,3}$ edges indicates a small positive

orbital magnetization that accounts to 0.011 to $0.014\mu_B$ per hole, showcasing an almost quenched orbital magnetic moment. This can be expected as the local symmetry of the metal center is only slightly disturbed by the addition of hydrogen atom with respect to the $[OMn^VO]^+$ complex. The quartet ground state identified from the experimental data is also in agreement with our ground state as determined by DFT, for details see the ESI.†

Despite the significantly different XMCD intensity in $[OMn^VO]^+$ and $[OMn^{IV}OH]^+$ complexes, there are only marginal differences in the XMCD spectral signatures of both molecules as can be seen from a direct comparison shown in ESI,† Fig. S9. Consequently, the fingerprint of the XMCD signal of high-valent manganese is less suitable for determining the respective electronic configuration and spin state. However, there is a distinct difference in their XAS spectral signature (see ESI,† Fig. S9) that is even more pronounced than in manganese with a local $3d^3$ and $3d^4$ electron configuration, respectively,[46] and might be used as a spectral fingerprint.

3.3 Energy level diagram and oxygen K-edge X-ray absorption spectra

Complementary to manganese $L_{2,3}$-edge X-ray absorption we also recorded oxygen K-edge X-ray absorption spectra, which are presented in the right panels of Fig. 2. In the absence of multiplet effects, X-ray absorption is a measure of the unoccupied density of states. Hence, we also show the oxygen p-projected density of states in Fig. 2 in comparison to the experimental oxygen K-edge absorption spectrum. The good agreement between the calculated density of states and the experimental data allows us to directly extract energy level diagrams as presented in the left panels of the same figure.[38] This has the advantage that we do not have to rely on simulations of oxygen K-edge spectra capitalizing on multiconfigurational self-consistent field wavefunction methods as recently reported.[47] The crystal field induced by the oxygen atoms lifts the degeneracy of the manganese 3d states and groups the molecular orbitals with significant 3d character.[48] In the $[OMn^VO]^+$ complex the aforementioned grouping nicely correlates with the orientation of the 3d-derived states relative to the ligand orbitals. Therefore, the two occupied α-spin molecular orbitals (MOs) $10a_1$ and $4b_1$ are grouped together and are separated from the $11a_1$ and $2a_2$ MOs by about 3.8 eV. The molecular orbital $7b_2$ with significant 3d electron density along the Mn–O axes experiences an additional energy penalty pushing it up in energy by another 1.5 eV. We in turn used these parameters as a starting point for further CF simulations of the manganese $L_{2,3}$-edge XAS and XMCD spectra. Again, the agreement between the resulting simulations and the experimental spectra remains poor as can be seen from ESI,† Fig. S7.

The energy separation of $10a_1$ and $4b_1$ of 0.2 eV is considerably smaller than the 3d exchange interaction of 0.45 eV (CASPT2/RASPT2.[13]) and 0.55 eV (DFT, B3LYP/def2-TZVP), respectively, as deduced from the singlet–triplet gap of $[OMn^VO]^+$, which is also consistent with the exchange splitting of 0.53 eV in atomic Ti^{2+} with $3d^2$ configuration.[50] This results

5832 | *Phys. Chem. Chem. Phys.*, 2024, **26**, 5830–5835
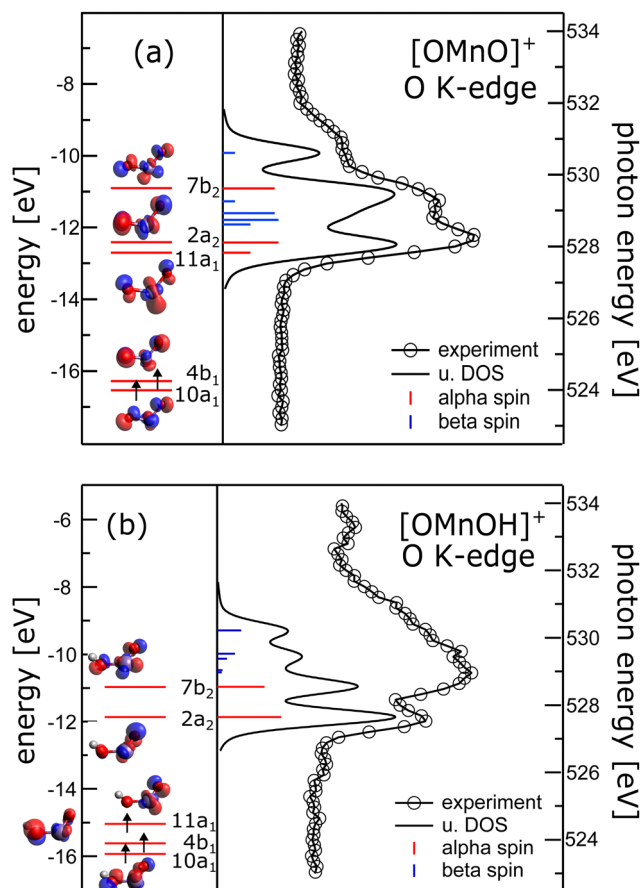
This journal is © the Owner Societies 2024

Fig. 2 Left panels: Energy level diagram deduced from α spins along isosurface plots of the molecular orbitals of (a) $[OMn^VO]^+$ and (b) $[OMn^{IV}OH]^+$ complexes. Arrows indicate occupied molecular orbitals. Right panel: Comparison of oxygen K-edge absorption (340 meV energy resolution) and oxygen p-projected density of states (broadened with a Gaussian of 0.3 eV full width half maximum and a 0.16 eV Lorentzian[49] to account for experimental resolution and core hole lifetime, respectively) of (a) $[OMn^VO]^+$ and (b) $[OMn^{IV}OH]^+$ complexes. Blue and red sticks show α and β spin states, respectively. For $[OMn^{IV}OH]^+$ we use the molecular orbital nomenclature in C_{2v} symmetry as the local symmetry at the metal is only slightly disturbed by the addition of the hydrogen atom. This allows for a more direct comparison to $[OMn^VO]^+$.

in the stabilization of the triplet ground state, also present in other isoelectronic high-valent transition metal dioxide molecules.[51–60]

In $[OMn^{IV}OH]^+$ with an overall C_s symmetry, the local symmetry at the manganese site deviates only slightly from C_{2v} symmetry. We therefore use the same nomenclature for the molecular orbitals as in $[OMn^VO]^+$. The crystal field splitting in $[OMn^{IV}OH]^+$ is less pronounced than in $[OMn^VO]^+$, but the molecular orbitals $10a_1$ and $4b_1$ remain grouped relatively close (0.3 eV) in energy, and $4b_1$ is separated from $11a_1$ by 0.58 eV. This splitting is still considerably smaller than the high-spin–low-spin transition energy of manganese with a $3d^3$ electronic configuration[46] resulting in the observed quartet spin state. As expected the molecular orbital $7b_2$ suffers an additional energy penalty relative to $2a_2$, which amounts to 0.9 eV. From the electron configuration of the $[OMn^{IV}OH]^+$ complex we deduce a $^4A''$ (C_s) ground state, which is identical to the reported ground state of isoelectronic $[OVOH]^-$.[61]

At the manganese site the local symmetry resembles neutral OMnO with similar Mn–O bond distances and angle of 1.603/1.699 Å, 123.5° in $[OMn^{IV}OH]^+$ compared to 1.639 Å, 118.4°[13] and 1.581 Å, 131°[62] in neutral OMnO. In C_{2v} symmetry the ground state of the $[OMn^{IV}OH]^+$ complex could be described as a $^4B_1$ state with $(10a_1)^1 (4b_1)^1 (11a_1)^1$ configuration, in agreement with the ground state reported for neutral OMnO by DFT,[52,53,56,62] but distinct from a $^4B_2$ ground state found by employing multiconfigurational wavefunction methods.[13] However, the latter differs from the former only by swapping the energetic ordering of the nearly degenerate $11a_1$ and $2a_2$ molecular orbitals. Furthermore, the leading line in the oxygen K-edge absorption of $[OMn^VO]^+$ was predicted to be reduced in neutral OMnO.[13] Indeed we observe a reduction in intensity of the low energy line when comparing $[OMn^VO]^+$ and $[OMn^{IV}OH]^+$ complexes further substantiating the similarity of $[OMn^{IV}OH]^+$ and neutral OMn^{IV}O. Note, that this reduction is not present in the oxygen p-projected density of states, which may also not be expected as this approach neglects any variation of the oscillator strength due to changing overlap of the 2p wavefunction and the involved molecular orbitals.

The XMCD and XAS spectra of $[OMn^{IV}OH]^+$ should be very similar to those of the neutral OMnO complex given their similar local electronic structure and symmetry. Therefore the XMCD and XAS spectra of $[OMn^{IV}OH]^+$ might be used as a spectral fingerprint for neutral OMnO.

Furthermore, we want to emphasize that neither in the oxygen K-edge spectrum of $[OMn^VO]^+$ nor in $[OMn^{IV}OH]^+$ the molecular orbital contributing to the energetically lowest lying excitation of the spectrum has a prominent 3d character. This is in contrast to the case of oxygen centered radicals,[63] which can therefore be excluded here.

4 Conclusion and outlook

Using XMCD spectroscopy we conclusively demonstrate that the ground state of the dioxidomanganese(v) cation is the high-spin state $^3B_1$ as foreshadowed by an earlier study employing experimental and computational XAS only.[13] Hence, we fully establish $[OMn^VO]^+$ as the second known manganese(v)-oxo complex to exhibit a high-spin ground state.[15,16] This is an important piece of information when considering reaction pathways involving high-valent species such as $[OMn^VO]^+$ that might well be intermediate species for which the spin state could be rate determining.

Furthermore, we present the first XMCD spectrum of a high-spin manganese(v) oxo complex, *i.e.*, of a high-spin manganese center in a local $3d^2$ electronic configuration. Reproducing the spectral signature properly is a challenge for both semi-empirical models – as demonstrated here but also for other $3d^2$ systems[40–42] – as well as for wavefunction-based *ab initio* electronic structure theory.[43] Nonetheless, considerable progress has been made by wavefunction-based *ab initio* methods in reproducing both XAS and XMCD signatures of transition

This journal is © the Owner Societies 2024

Phys. Chem. Chem. Phys., 2024, **26**, 5830–5835 | **5833**

metal compounds and will become invaluable in interpreting experimental data.

Moreover, we also provide the XAS and XMCD spectrum for the high-spin hydroxidooxidomanganese(IV) cation with almost identical local symmetry at the manganese site as in $[OMnO]^{+,0}$. Manganese centers in both, oxidation states +4 and +5, might play a significant role in the oxygen evolving reaction of photosystem II. Hence, the reported spectra can serve as a benchmark not only for studying the OEC but also for studying other multinuclear manganese systems[64,65] and to further refine quantum chemical methods.

However, what remains elusive is the existence of a high-valent–high-spin species in a multinuclear manganese complex, which is an issue closely intertwined with important oxidation reactions such as the Kok cycle.[66] We hope that this study will encourage future studies into such systems.

Author contributions

JTL, OSA, and VZB devised the project, designed the experimental study, and prepared the beamtime proposal. JTL, KH, and VZB designed the experimental setup. MF, MSS, OSA and VZB performed the experiments, and validated their reproducibility. OSA analyzed the data under guidance of JTL, KH, and VZB. OSA, KH and VZB performed the calculations. JTL, KH, and VZB supervised the project. OSA wrote the original draft, with reviewing and editing by JTL, KH, and VZB.

Conflicts of interest

There are no conflicts to declare.

Acknowledgements

Notes and references

1 V. A. Larson, B. Battistella, K. Ray, N. Lehnert and W. Nam, *Nat. Rev. Chem.*, 2020, **4**, 404–419.

2 X. P. Zhang, A. Chandra, Y. M. Lee, R. Cao, K. Ray and W. Nam, *Chem. Soc. Rev.*, 2021, **50**, 4804–4811.

3 T. Yang, M. G. Quesne, H. M. Neu, F. G. Cantú Reinhard, D. P. Goldberg and S. P. de Visser, *J. Am. Chem. Soc.*, 2016, **138**, 12375–12386.

4 Z. Chen and G. Yin, *Chem. Soc. Rev.*, 2015, **44**, 1083–1100.

5 V. Krewald, M. Retegan, F. Neese, W. Lubitz, D. A. Pantazis and N. Cox, *Inorg. Chem.*, 2016, **55**, 488–501.

6 X.-X. Li, M. Guo, B. Qiu, K.-B. Cho, W. Sun and W. Nam, *Inorg. Chem.*, 2019, **58**, 14842–14852.

7 J. Barber, *Nat. Plants*, 2017, **3**, 17041.

8 N. Cox, D. A. Pantazis and W. Lubitz, *Annu. Rev. Biochem.*, 2020, **89**, 795–820.

9 S. H. Kim, H. Park, M. S. Seo, M. Kubo, T. Ogura, J. Klajn, D. T. Gryko, J. S. Valentine and W. Nam, *J. Am. Chem. Soc.*, 2010, **132**, 14030–14032.

10 Y. Guo, J. Messinger, L. Kloo and L. Sun, *J. Am. Chem. Soc.*, 2023, **145**, 4129–4141.

11 V. Krewald, F. Neese and D. A. Pantazis, *J. Inorg. Biochem.*, 2019, **199**, 110797.

12 H. M. Neu, R. A. Baglia and D. P. Goldberg, *Acc. Chem. Res.*, 2015, **48**, 2754–2764.

13 M. G. Delcey, R. Lindblad, M. Timm, C. Bülow, V. Zamudio-Bayer, B. von Issendorff, J. T. Lau and M. Lundberg, *Phys. Chem. Chem. Phys.*, 2022, **24**, 3598–3610.

14 D. Feichtinger and D. A. Plattner, *Angew. Chem., Int. Ed. Engl.*, 1997, **36**, 1718–1719.

15 T. Taguchi, R. Gupta, B. Lassalle-Kaiser, D. W. Boyce, V. K. Yachandra, W. B. Tolman, J. Yano, M. P. Hendrich and A. S. Borovik, *J. Am. Chem. Soc.*, 2012, **134**, 1996–1999.

16 R. Gupta, T. Taguchi, B. Lassalle-Kaiser, E. L. Bominaar, J. Yano, M. P. Hendrich and A. S. Borovik, *Proc. Natl. Acad. Sci. U. S. A.*, 2015, **112**, 5319–5324.

17 M. Niemeyer, K. Hirsch, V. Zamudio-Bayer, A. Langenberg, M. Vogel, M. Kossick, C. Ebrecht, K. Egashira, A. Terasaki, T. Möller, B. V. Issendorff and J. T. Lau, *Phys. Rev. Lett.*, 2012, **108**, 57201.

18 V. Zamudio-Bayer, K. Hirsch, A. Langenberg, M. Kossick, A. Ławicki, A. Terasaki, B. V. Issendorff and J. T. Lau, *J. Chem. Phys.*, 2015, **142**, 234301.

19 V. Zamudio-Bayer, K. Hirsch, A. Langenberg, M. Niemeyer, M. Vogel, A. Ławicki, A. Terasaki, J. T. Lau and B. von Issendorff, *Angew. Chem., Int. Ed.*, 2015, **54**, 4498–4501.

20 A. Langenberg, K. Hirsch, A. Ławicki, V. Zamudio-Bayer, M. Niemeyer, P. Chmiela, B. Langbehn, A. Terasaki, B. V. Issendorff and J. T. Lau, *Phys. Rev. B: Condens. Matter Mater. Phys.*, 2014, **90**, 184420.

21 K. Hirsch, J. T. Lau, P. Klar, A. Langenberg, J. Probst, J. Rittmann, M. Vogel, V. Zamudio-Bayer, T. Möller and B. von Issendorff, *J. Phys. B: At., Mol. Opt. Phys.*, 2009, **42**, 154029.

22 E. Stavitski and F. M. F. de Groot, *Micron*, 2010, **41**, 687–694.

23 J. Fernandez-Rodriguez, B. Toby and M. Van Veenendaal, *J. Electron Spectrosc. Relat. Phenom.*, 2015, **202**, 81–88.

24 F. Neese, *WIREs Comput. Mol. Sci.*, 2012, **2**, 73–78.

25 A. D. Becke, *J. Chem. Phys.*, 1993, **98**, 5648–5652.

26 P. J. Stephens, F. J. Devlin, C. F. Chabalowski and M. J. Frisch, *J. Phys. Chem.*, 1994, **98**, 11623–11627.

27 K. Eichkorn, F. Weigend, O. Treutler and R. Ahlrichs, *Theor. Chem. Acc.*, 1997, **97**, 119–124.

28 M. Flach, K. Hirsch, M. Timm, O. S. Ablyasova, M. D. S. Santos, M. Kubin, C. Bülow, T. Gitzinger, B. von Issendorff, J. T. Lau and V. Zamudio-Bayer, *Phys. Chem. Chem. Phys.*, 2022, **24**, 19890–19894.

5834 | *Phys. Chem. Chem. Phys.*, 2024, **26**, 5830–5835

This journal is © the Owner Societies 2024

29 M. R. A. Blomberg and P. E. M. Siegbahn, *Theor. Chem. Acc.*, 1997, **97**, 72–80.

30 B. T. Thole, P. Carra, F. Sette and G. van der Laan, *Phys. Rev. Lett.*, 1992, **68**, 1943.

31 P. Carra, B. T. Thole, M. Altarelli and X. Wang, *Phys. Rev. Lett.*, 1993, **70**, 694.

32 C. T. Chen, Y. U. Idzerda, H.-J. Lin, N. V. Smith, G. Meigs, E. Chaban, G. H. Ho, E. Pellegrin and F. Sette, *Phys. Rev. Lett.*, 1995, **75**, 152.

33 G. F. Dionne, *Magnetic Oxides*, Springer US, Boston, MA, 2009.

34 F. M. F. de Groot, *Coord. Chem. Rev.*, 2005, **249**, 31–63.

35 F. M. F. de Groot, *J. Electron Spectrosc. Relat. Phenom.*, 1994, **67**, 529–622.

36 S. P. Cramer, F. M. F. DeGroot, Y. Ma, C. T. Chen, F. Sette, C. A. Kipke, D. M. Eichhorn, M. K. Chan, W. H. Armstrong, E. Libby, G. Christou, S. Brooker, V. McKee, O. C. Mullins and J. C. Fuggle, *J. Am. Chem. Soc.*, 1991, **113**, 7937–7940.

37 M. Risch, K. A. Stoerzinger, B. Han, T. Z. Regier, D. Peak, S. Y. Sayed, C. Wei, Z. Xu and Y. Shao-Horn, *J. Phys. Chem. C*, 2017, **121**, 17682–17692.

38 O. S. Ablyasova, M. Guo, V. Zamudio-Bayer, M. Kubin, T. Gitzinger, M. da Silva Santos, M. Flach, M. Timm, M. Lundberg, J. T. Lau and K. Hirsch, *J. Phys. Chem. A*, 2023, **127**, 7121–7131.

39 C. Piamonteze, P. Miedema and F. M. F. de Groot, *Phys. Rev. B: Condens. Matter Mater. Phys.*, 2009, **80**, 184410.

40 D. Hovančík, J. Pospíšil, K. Carva, V. Sechovský and C. Piamonteze, *Nano Lett.*, 2023, **23**, 1175–1180.

41 R. Sant, A. D. Vita, V. Polewczyk, G. M. Pierantozzi, F. Mazzola, G. Vinai, G. van der Laan, G. Panaccione and N. B. Brookes, *J. Phys.: Condens. Matter*, 2023, **35**, 405601.

42 J.-S. Kang, J. Hwang, D. H. Kim, E. Lee, W. C. Kim, C. S. Kim, S. Kwon, S. Lee, J.-Y. Kim, T. Ueno, M. Sawada, B. Kim, B. H. Kim and B. I. Min, *Phys. Rev. B: Condens. Matter Mater. Phys.*, 2012, **85**, 165136.

43 D. Maganas, J. K. Kowalska, C. Van Stappen, S. DeBeer and F. Neese, *J. Chem. Phys.*, 2020, **152**, 114107.

44 A. Frisk, L. B. Duffy, S. Zhang, G. van der Laan and T. Hesjedal, *Mater. Lett.*, 2018, **232**, 5–7.

45 A. Ghosh, H. J. M. Jönsson, D. J. Mukkattukavil, Y. Kvashnin, D. Phuyal, P. Thunström, M. Agåker, A. Nicolaou, M. Jonak, R. Klingeler, M. V. Kamalakar, T. Sarkar, A. N. Vasiliev, S. M. Butorin, O. Eriksson and M. Abdel-Hafiez, *Phys. Rev. B: Condens. Matter Mater. Phys.*, 2023, **107**, 115148.

46 G. van der Laan and B. T. Thole, *J. Phys.: Condens. Matter*, 1992, **4**, 4181.

47 M. Scott and M. G. Delcey, *J. Chem. Theory Comput.*, 2023, **19**, 5924–5937.

48 F. Habib, O. R. Luca, V. Vieru, M. Shiddiq, I. Korobkov, S. I. Gorelsky, M. K. Takase, L. F. Chibotaru, S. Hill, R. H. Crabtree and M. Murugesu, *Angew. Chem., Int. Ed.*, 2013, **52**, 11290–11293.

49 M. Coreno, M. de Simone, K. C. Prince, R. Richter, M. Vondráček, L. Avaldi and R. Camilloni, *Chem. Phys. Lett.*, 1999, **306**, 269–274.

50 E. B. Saloman, *J. Phys. Chem. Ref. Data*, 2012, **41**, 013101.

51 G. V. Chertihin, W. D. Bare and L. Andrews, *J. Phys. Chem. A*, 1997, **101**, 5090–5096.

52 G. L. Gutsev, B. K. Rao and P. Jena, *J. Phys. Chem. A*, 2000, **104**, 11961–11971.

53 E. L. Uzunova, H. Mikosch and G. S. Nikolov, *J. Chem. Phys.*, 2008, **128**, 094307.

54 F. Grein, *Chem. Phys.*, 2008, **343**, 231–240.

55 Y. Wang, X. Gong and J. Wang, *Phys. Chem. Chem. Phys.*, 2010, **12**, 2471–2477.

56 Y. Gong, M. Zhou and L. Andrews, *Chem. Rev.*, 2009, **109**, 6765–6808.

57 G. L. Gutsev, P. Jena, H.-J. Zhai and L.-S. Wang, *J. Chem. Phys.*, 2001, **115**, 7935–7944.

58 P. B. Armentrout, *J. Chem. Phys.*, 2013, **139**, 084305.

59 M. Zhou and L. Andrews, *J. Chem. Phys.*, 1999, **111**, 4230–4238.

60 J. Gancheff, C. Kremer, E. Kremer and O. N. Ventura, *J. Mol. Struct. THEOCHEM*, 2002, **580**, 107–116.

61 Y. Wang, C. Han, J. Hong, Z. Fei, C. Dong, H. Liu and X. Xiong, *RSC Adv.*, 2021, **11**, 18729–18736.

62 G. V. Chertihin and L. Andrews, *J. Phys. Chem. A*, 1997, **101**, 8547–8553.

63 M. da Silva Santos, R. Medel, M. Flach, O. S. Ablyasova, M. Timm, B. von Issendorff, K. Hirsch, V. Zamudio-Bayer, S. Riedel and J. T. Lau, *Chem. Phys. Chem.*, 2023, e202300390.

64 M. Mannini, P. Sainctavit, R. Sessoli, C. Cartier dit Moulin, F. Pineider, M.-A. Arrio, A. Cornia and D. Gatteschi, *Chem. – Eur. J.*, 2008, **14**, 7530–7535.

65 M. Tombers, J. Meyer, J. Meyer, A. Lawicki, V. Zamudio-Bayer, K. Hirsch, J. T. Lau, B. von Issendorff, A. Terasaki, T. A. Schlathölter, R. A. Hoekstra, S. Schmidt, A. K. Powell, E. Kessler, M. H. Prosenc, C. van Wüllen and G. Niedner-Schatteburg, *Chem. – Eur. J.*, 2022, **28**, e202102592.

66 B. Kok, B. Forbush and M. McGloin, *Photochem. Photobiol.*, 1970, **11**, 457–475.

This journal is © the Owner Societies 2024

Phys. Chem. Chem. Phys., 2024, **26**, 5830–5835 | **5835**